

Principle and performance analysis of the Levenberg-Marquardt algorithm in WMS spectral line fitting

YONGJIE SUN,^{1,2} TINTING ZHANG,¹ KUN LI,² PENGPENG WANG,¹ FENG PENG,² AND CUNGUANG ZHU^{1,*}

¹ School of Physical Science and Information Technology, Liaocheng University, Liaocheng 252000, China

² School of Physical Science and Technology, University of Jinan, Jinan 250022, China

*Corresponding author: zhucunguang@lcu.edu.cn

Abstract: Calibration-free wavelength modulation spectroscopy (WMS) is an efficient technique for trace gas monitoring. It is widely used due to its resistance to light intensity fluctuations, strong suppression of low-frequency noise, fast response time and excellent environmental adaptability. The calibration-free WMS often employs the Levenberg-Marquardt algorithm for spectral fitting to retrieve gas characteristics. However, to the best of our knowledge, an analysis of the main factors affecting the operational effectiveness of the Levenberg-Marquardt algorithm in calibration-free WMS has merely been reported. In this paper, we have systematically analyzed the Levenberg-Marquardt algorithm's operating mechanism in WMS- $2f/1f$. The simulation results show that the number of parameters and initial parameter estimated errors are the main factors limiting the retrieval accuracy of the algorithm.

© 2021 Optica Publishing Group under the terms of the [Optica Publishing Group Open Access Publishing Agreement](#)

1. INTRODUCTION

Wavelength modulation spectroscopy (WMS) is a non-contact technique for trace gas monitoring, which is widely used due to its high sensitivity and fast dynamic response[1-5]. In conventional WMS, the measurement signal requires calibration with a gas mixture of known concentrations, which limits the application of WMS technology in harsh environments (high temperature or pressure) or where the relevant gas conditions are poorly known.

Researchers have recently developed numerous calibration-free techniques to address this issue [6-12]. Li et al. [13] developed a simulating WMS analytical model as a function of easily obtainable laser parameters and an absorption spectrum. This method can eliminate the majority of calibration factors and infer gas parameters. Rieker et al. [14] utilized the first harmonics to normalize the second harmonics (WMS- $2f/1f$) and extended the WMS analysis model to the field of combustion monitoring to retrieve the temperature and concentration of water vapor simultaneously. Our research group [15] has proposed a sensitive second harmonic phase angle measurement method capable of background-free gas monitoring. However, the retrieval accuracy of gas parameters using these techniques generally depends on the comprehensive characterization of the target transition's line shape parameters (such as collisional broadening coefficients) and the laser parameters, which typically require extensive laboratory work. This challenge can be avoided by using the methodology of Christopher et al. [16]. They set the target transition's line shape parameters and the gas concentration as parameters to be estimated and used the Levenberg-Marquardt (LM) algorithm to perform spectral line fitting to retrieve the gas's condition. Due to its lower requirements for line shape and laser parameters characterization, this LM methodology has been extensively used for highly sensitive and robust measurements of gas conditions. Combining the LM algorithm with dual-spectroscopy techniques, Li et al.[17] developed a mid-infrared laser trace gas sensor capable of online

monitoring the concentration of multi-component gases. Yipeng Zang et al. [18] proposed a method to retrieve high-temperature spectral line parameters using the LM algorithm for least-squares fitting absorption spectra in the combustion flow field. Raza et al.[19] developed a dual-species (CO/NH₃) sensor based on the LM methodology for high-temperature measurements. However, an analysis of the main factors affecting the operational effectiveness of the LM algorithm in calibration-free WMS has merely been reported. In this paper, we have systematically analyzed the Levenberg-Marquardt algorithm's operating mechanism in WMS-2f/1f.

2. METHODOLOGY

2.1 WMS-2f/1f Theoretical Model

The injected current of the laser diode is periodically modulated by a high-frequency sinusoidal signal to produce an instantaneous optical frequency $\nu(t)$ and light intensity $I_0(t)$:

$$\nu(t) = \nu + \Delta\nu\cos(\omega t) \quad (1)$$

$$I_0(t) = \bar{I}_0 \left(1 + i_1 \cos(\omega t + \psi_1) + i_2 \cos(2\omega t + \psi_2) \right) \quad (2)$$

where ν is the laser center frequency, $\Delta\nu$ is the modulation depth, \bar{I}_0 is the average light intensity, i_1 and i_2 are the intensity amplitudes of the first- and second-order (normalized by \bar{I}_0), ψ_1 is the FM/IM phase shift, and ψ_2 is the phase shift between the FM and the nonlinear IM.

According to the Beer-Lambert law, the spectroscopic absorbance can be written as:

$$\tau(\nu(t)) = \frac{I(t)}{I_0(t)} = \exp[-PCLS(T)\Phi_\nu] = \exp[-A\phi_\nu] \quad (3)$$

where $I(t)$ and $I_0(t)$ are the transmitted and incident laser intensities, P is the total gas pressure, $S(T)$ is the strength of absorption line at T temperature, Φ_ν is a line-shape function of the absorption spectrum of the gas, C is the concentration of the gas to be measured, L is the length of the optical range, A is the integrated absorbance.

The $\tau(\nu(t))$ can be expanded in a Fourier cosine series, where the H term as follows:

$$H_0(\nu(t)) = \frac{1}{2\pi} \int_{-\pi}^{\pi} \tau(\nu(t)) d\theta \quad (4)$$

$$H_k(\nu(t)) = \frac{1}{\pi} \int_{-\pi}^{\pi} \tau(\nu(t)) \cos(k\theta) d\theta \quad (5)$$

The $I(t)$ signal is input into the lock-in amplifier (LIA) to extract the X_{nf} and Y_{nf} to determine $S_{2f/1f}$, given by Eq. (6):

$$\begin{aligned} \text{WMS-2f/1f} &= \sqrt{\left(\frac{X_{2f}}{X_{1f}}\right)^2 + \left(\frac{Y_{2f}}{Y_{1f}}\right)^2} \\ &= \sqrt{\left(\frac{H_2 + \frac{i_1}{2}(H_1 + H_3)\cos\psi_1 + i_2 H_0 \cos\psi_2}{H_1 + i_1\left(H_0 + \frac{H_2}{2}\right)\cos\psi_1 + \frac{i_2}{2}(H_1 + H_3)\cos\psi_2}\right)^2 + \left(\frac{\frac{i_1}{2}(H_1 - H_3)\sin\psi_1 + i_2 H_0 \sin\psi_2}{i_1\left(H_0 - \frac{H_2}{2}\right)\sin\psi_1 + \frac{i_2}{2}(H_1 - H_3)\sin\psi_2}\right)^2} \\ &= F(A, m, i_1, i_2, \psi_1, \psi_2) \end{aligned} \quad (6)$$

From Eq. (6), it is clear that the WMS-2f/1f spectral model is a function of transition integrated absorbance and laser tuning parameters. For an isolated absorption line, the modulation index

m is defined by $2\Delta\nu / \Delta\nu_c$, where $\Delta\nu_c$ is the full width at half maximum (FWHM) of the gas absorption line.

2.2 LM Algorithm Overview

The LM algorithm is a classical optimization algorithm between the Steepest Gradient Descent method and the Gaussian Newton method. Its fundamental concept is to optimize the nonlinear least squares problems by performing differentiation operations on the artificial initialization parameters [20].

The LM-based spectral fitting technique aims to find the optimal solution β to minimize the error function between the simulated and measured spectra. The expression of the error function z is described as follows:

$$z = \min_{\beta \in R} \sum_{i=1}^N \|F_i(\beta) - y_i\|^2 \quad (7)$$

Where $i=1,2,3,\dots, N$ (Given a spectral data set), $F(\beta)$ is the simulated WMS $-2f/1f$ spectrum given by Eq. (6), and y is the measured spectrum. The LM algorithm updates the parameter β with the coefficient matrix $(J^T J + \mu I)$ along the negative gradient direction, and the parameters update equation can be described as:

$$\beta_d^{t+1} = \beta_d^t - (J^T J + \mu I)^{-1} J^T z \quad (8)$$

where $d=1,2,3,\dots, D$ (estimated parameters), $t+1$ denotes the $t+1$ th iteration, I denotes the unit matrix, μ is the damping coefficient, $J^T z$ is the gradient, $J^T J$ approximates the Hessian matrix; the Jacobian J of a function $F: R^D \rightarrow R^N$ is the matrix of its first partial derivatives.

$$J = \begin{bmatrix} \frac{\partial F_1}{\partial \beta_1} & \dots & \frac{\partial F_1}{\partial \beta_D} \\ \vdots & \ddots & \vdots \\ \frac{\partial F_N}{\partial \beta_1} & \dots & \frac{\partial F_N}{\partial \beta_D} \end{bmatrix} \quad (9)$$

2.3 The Design Process of LM-based Spectral Fitting Technique

The laser tuning parameter in $F(\beta)$ can be characterized in the laboratory according to the procedures in [13], or the laser tuning parameter and the integrated absorbance can be set together as estimated parameters, and the absorption information of gas can be obtained by the LM fit between the measured and simulated spectrum. In the optimization process, β is defined as $\beta = [m, A, i_1, i_2, \psi_1, \psi_2]$.

Step 1: Initial weights. The initial parameter estimates β , let the number of iterations $t=0$, adjustment coefficient μ and error tolerance ε were set.

Step 2: The Jacobian matrix J is calculated according to the current parameters.

Step 3: During iterative optimization, the parameter β^{t+1} is updated by Eq. (8).

Step 4: Based on the updated parameters, the error between the simulated and the measured spectral is recalculated. If $z > \varepsilon$, adjust the damping factor μ and return to Step 2. Otherwise, the iteration is terminated, and the results are output.

The flow chart of LM-based spectral fitting for extracting gas absorption information is shown in Fig. 1. Once the fitting routine has converged, the best-fit integrated absorbance A is used to calculate the gas concentration.

$$C_{\text{Sim}} = \frac{A}{PS(T)L} \quad (10)$$

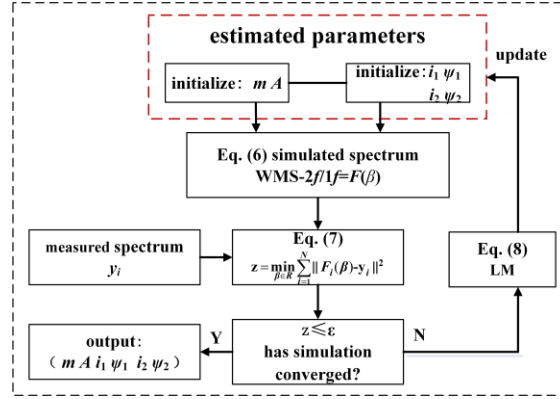


Fig. 1. Flow chart of LM-based spectral fitting

3. SIMULATION RESULTS AND ANALYSIS

This section analyzes the main factors affecting the operational effectiveness of the LM algorithm in the WMS-2f/1f system using the MATLAB R2019b simulation software. In this case, the computer has the following specifications: CPU:i5-10400F; RAM: 8GB.

The P(13) spectral line of acetylene gas at 1532.83 nm was selected as the simulation target spectral line and periodically scanned to collect a set of reference data, recorded as y . The main parameters used in the simulation are listed in Table 1.

Table 1. List of Model Parameters

Parameters	Accurate value
C [ppmv]	296
i_1	0.20
i_2	3×10^{-3}
ψ_1 [π]	1.60
ψ_2 [π]	1.50
m [cm^{-1}]	1.43
$\Delta\nu_2$ [$\text{cm}^{-1}/\text{atm}$]	0.0777

In order to better analyze and evaluate the main factors affecting the operational effectiveness of the LM algorithm in the WMS-2f/1f system, the concentration relative error C_δ , the fitting degree H , and convergence time are introduced. The calculation equations are shown in Eq. (11) and Eq. (12), respectively. It can be seen from the equation that the smaller concentration relative error and the degree of fit, the closer the fitted value is to the actual value, and the better the operational effectiveness of the LM algorithm.

$$H = \sum_{i=1}^N (F_i - y_i)^2 \quad (11)$$

$$C_\delta = \frac{|C_{\text{Sim}} - C|}{C} \times 100\% \quad (12)$$

3.1 Effect of the Number of Estimated Parameters

The effect of the number of estimated parameters in the WMS-2f/1f model on the operational effectiveness of the LM algorithm for concentration retrieval is analyzed. Fig. 2

shows that when the number of estimated parameters in WMS-2f/1f model increases from 2 to 6 (the integrated absorbance A is fixed as the estimated parameter), the concentration relative error curve increases nonlinearly. The specific comparison results are shown in Table 2.

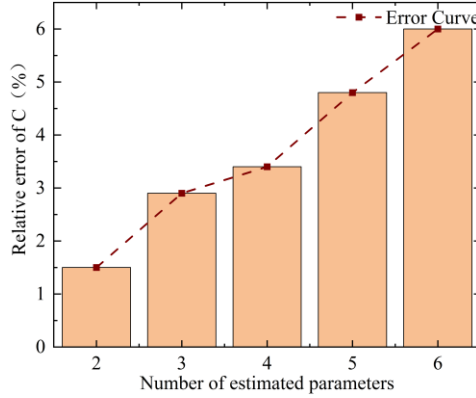


Fig. 2. The concentration relative error curve under different numbers of parameters in model.

Table 2 shows a negative correlation between the operational performance of the LM algorithm and the number of estimated parameters in WMS-2f/1f model. For two estimated parameters (other parameters not listed are the accurate values), C_s is 1.5%, H is 3.2×10^{-8} , and the convergence time is 104 s. The overall operating performance of the LM algorithm is good, and the LM-based spectral fitting technique can measure the gas concentration with high accuracy. With the increase in the number of estimated parameters, it can be seen from the Table 2 comparison results that the LM algorithm operation performance gradually worsens. In the case of 6 evaluated parameters, C_s is 6.0%, H is 3.0×10^{-3} , and the convergence time is 236 s. The overall operating performance of the LM algorithm is poor. At this time, the LM-based spectral fitting technique cannot meet the demand of measuring concentration with high accuracy.

Table 2. Comparison Results under Different Number of Estimated Parameters

Estimated parameters	Concentration relative error C_s (%)	Fitting degree H	Convergence time (s)
2 [m, A]	1.5	3.2×10^{-8}	104
3 [m, i_1, A]	2.9	8.7×10^{-7}	140
4 [m, i_1, i_2, A]	3.4	5.4×10^{-6}	173
5 [m, i_1, i_2, ψ_1, A]	4.8	1.9×10^{-5}	201
6 [$m, i_1, i_2, \psi_1, \psi_2, A$]	6.0	3.0×10^{-3}	236

The reason for this situation may be related to the change in the size of the Jacobian matrix J of Eq. (9). The matrix size of the Jacobian matrix J , which is the first-order partial derivative matrix of the function F , increases with the number of estimated parameters. This matrix size variation directly leads to an increase in the computational dimensionality of $(J^T J + \mu I)$ and $J^T z$ in the parameter update equation of Eq. (8), which ultimately affects the operational performance of the LM algorithm for concentration monitoring.

3.2 Effect of Initial Parameter Estimated Errors

The operational effectiveness of the LM algorithm for concentration retrieval under different initial parameter estimated errors (absolute error between the initial parameter estimate value and the accurate value) is analyzed. Fig. 3 shows that the concentration relative error curve increases with the initial parameter estimated errors.

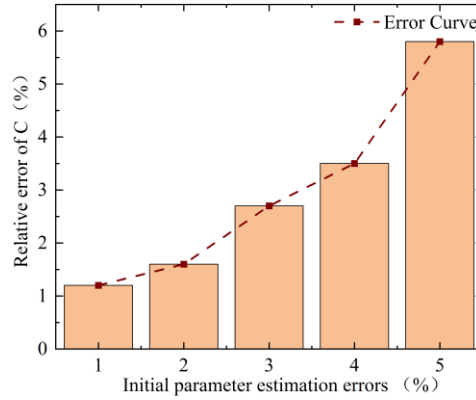


Fig. 3. The concentration relative error curve under different initial parameter estimated errors.

According to Table 3, a negative correlation exists between the operational performance of the LM algorithm and the initial parameter estimation errors. In the case of 1% initial parameter estimation errors, C_δ is 1.2%, and H is 3.6×10^{-12} . The overall operating performance of the LM algorithm is good. In the case of 5% initial parameters estimation errors, C_δ is 5.8%, and H is 1.4×10^{-9} . Compared with the 1% estimation error case, C_δ increases about 5 times, and H decreases by 3 orders of magnitude. The overall operating performance of the LM algorithm is poor.

Table 3. Comparison Results with Different Initial Parameter Estimated Errors

Initial parameter estimated errors/%	Concentration relative error C_δ (%)	Fitting degree H	Convergence time (s)
1	1.2	3.6×10^{-12}	243
2	1.6	1.6×10^{-11}	241
3	2.7	4.2×10^{-11}	239
4	3.5	8.2×10^{-11}	238
5	5.8	1.4×10^{-9}	244

The reason for this situation may be as follows: when the initial parameter estimation errors are small, the initial parameter estimates values are sufficiently close to the accurate values. The Gaussian Newton algorithm with second-order convergence performance dominates the LM algorithm. The Taylor expansion of the function F ignores the higher-order derivatives of the estimation errors, making a linear approximation in the neighborhood of the initial parameter estimates values and converting the nonlinear least squares problem into a linear least squares problem for the optimal solution β . The comparison results in Table 3 (estimation errors $\leq 4\%$) show that the overall operating performance of the LM algorithm is good. In the opposite case, When the initial parameter estimation error is large, the initial parameter estimates values are far from the accurate values. The higher-order derivative term of the estimation error is difficult to ignore. Then, the Steepest Gradient Descent algorithm with first-order convergence performance dominates the LM algorithm. The comparison results in Table 3 show that the LM algorithm performs poorly in the operation of concentration monitoring.

4. CONCLUSION

This paper analyzes the operational effectiveness of the LM algorithm in the WMS-2f/1f calibration-free system in terms of the number of estimated parameters and initial parameter estimated errors. The results show that both the number of parameters and the initial parameter estimated errors have a negative relationship with the operational performance of the LM

algorithm. When the function F contains two estimated parameters, C_δ is 1.5%, H is 3.2×10^{-8} , and the convergence time is 104 s. The overall performance of the LM algorithm is good. As the number of estimated parameters included in function F increases, the overall operational performance of the LM algorithm gradually becomes worse.

Similarly, with an initial parameter estimation error of 1%, C_δ of 1.2%, and H of 3.6×10^{-12} . The overall operating performance of the LM algorithm is good. At the initial parameter estimation error of 5%, compared to the case of the estimation error of 1%, at this time, C_δ increases by about 5 times and H decreases by 3 orders of magnitude, and the overall operation of the LM algorithm performs poorly from the comparison results. It is worth noting that there are more estimated parameters in the fitting routine, although it means that the LM algorithm will perform worse; currently, the workload of characterization will be reduced; on the contrary, fewer estimated parameters in the fitting routine, although it means that the workload of characterization will increase, the overall performance of the LM algorithm will be better. Therefore, the number of estimated parameters and the initial parameter estimated errors need to compromise the operational effectiveness of this algorithm and the characterization's workload.

Funding. National Natural Science Foundation of China (61705080); Promotive Research Fund for Excellent Young and Middle-aged Scientists of Shandong Province (ZR2016FB17, BS2015DX005); the Youth Innovation Technology Support Program of Shandong Province Colleges and Universities under Grant(2019KJJ011); Scientific Research Foundation of Liaocheng University (318012101); Startup Foundation for Advanced Talents of Liaocheng University (318052156,318052157).

Disclosures. The authors declare no conflicts of interest.

Data availability. Data underlying the results presented in this paper are not publicly available at this time but may be obtained from the authors upon reasonable request.

REFERENCES

1. Y. Du, L. Lan, Y. Ding, and Z. Peng, "Measurement of the absolute absorbance based on wavelength modulation spectroscopy," *Appl. Phys. B* **123**, 1–11 (2017).
2. Y. Du, Z. Peng, and Y. Ding, "Wavelength modulation spectroscopy for recovering absolute absorbance," *Opt. Express* **26**, 9263–9272 (2018).
3. R. Cui, L. Dong, H. Wu, S. Li, L. Zhang, W. Ma, W. Yin, L. Xiao, L. Jia and F. K. Tittel, "Highly sensitive and selective CO sensor using a 2.33 μm diode laser and wavelength modulation spectroscopy," *Opt. Express* **26**, 24318–24328 (2018).
4. C. Zhu, T. Chu, Y. Liu, and P. Wang, "Modeling of Scanned Wavelength Modulation Spectroscopy Considering Nonlinear Behavior of Intensity Response," *IEEE Sensors J.* **22**, 2301–2308 (2021).
5. J. Xia, F. Zhu, J. Bounds, E. Aluaee, A. Kolomenskii, Q. Dong, J. He, C. Meadows, S. Zhang and H. Schuessler, "Spectroscopic trace gas detection in air-based gas mixtures: Some methods and applications for breath analysis and environmental monitoring," *J. Appl. Phys.* **131**, 220901 (2022).
6. K. Duffin, A. James. McGettrick, W. Johnstone, G. Stewart, and D. G. Moodie, "Tunable diode-laser spectroscopy with wavelength modulation: a calibration-free approach to the recovery of absolute gas absorption line shapes," *J. Light. Technol.* **25**, 3114–3125 (2007).
7. Z. Qu, R. Ghorbani, D. Valiev, and F. M. Schmidt, "Calibration-free scanned wavelength modulation spectroscopy—application to H₂O and temperature sensing in flames," *Opt. Express* **23**, 16492–16499 (2015).
8. A. Behera, and A. Wang, "Calibration-free wavelength modulation spectroscopy: symmetry approach and residual amplitude modulation normalization," *Appl. Opt.* **55**, 4446–4455 (2016).
9. A. Upadhyay, D. Wilson, M. Lengden, A. L. Chakraborty, G. Stewart, and W. Johnstone, "Calibration-free WMS using a cw-DFB-QCL, a VCSEL, and an edge-emitting DFB laser with in-situ real-time laser parameter characterization," *IEEE Photonics J.* **9**, 1–17 (2017).
10. C. Yang, L. Mei, H. Deng, Z. Xu, B. Chen, and R. Kan, "Wavelength modulation spectroscopy by employing the first harmonic phase angle method," *Opt. Express* **27**, 12137–12146 (2019).
11. A. Roy, and A. Lal. Chakraborty, "Intensity modulation-normalized calibration-free $1f$ and $2f$ wavelength modulation spectroscopy," *IEEE Sensors J.* **20**, 12691–12701 (2020).
12. R. Li, F. Li, X. Lin, X. W. Shi, W. Huang, L. Li, and Z. Yang, "Linear calibration-free wavelength modulation spectroscopy," *Microw. Opt. Technol. Lett.* **04**, (2021).
13. H. Li, G. B. Rieker, X. Liu, J. B. Jeffries, and R. K. Hanson, "Extension of wavelength-modulation spectroscopy to large modulation depth for diode laser absorption measurements in high-pressure gases," *Appl. Opt.* **45**, 1052–1061 (2006).

14. G.B.Rieker, J.B.Jeffries, and R.K.Hanson, "Calibration-free wavelength-modulation spectroscopy for measurements of gas temperature and concentration in harsh environments," *Appl. Opt.* **48**, 5546–5560 (2009).
15. C. Zhu, P. Wang, T. Chu, F. Peng, and Y. Sun, "Second Harmonic Phase Angle Method Based on WMS for Background-Free Gas Detection," *IEEE Photonics J.* **13**, 1–6 (2021).
16. C. S. Goldenstein, C. L. Strand, I. A. Schultz, K. Sun, J. B. Jeffries, and R. K. Hanson, "Fitting of calibration-free scanned-wavelength-modulation spectroscopy spectra for determination of gas properties and absorption line shapes," *Appl. Opt.* **53**, 356–367 (2014).
17. J. Li, H. Deng, J. Sun, B. Yu, and H. Fischer, "Simultaneous atmospheric CO, N₂O and H₂O detection using a single quantum cascade laser sensor based on dual-spectroscopy techniques," *Sensors Actuators B: Chem.* **231**, 723–732 (2016).
18. Y. Zang, Z. Xu, H. Xia, A. Huang, Y. He, and R. Kan, "Method for Measuring High Temperature Spectral Line Parameters Based on Calibration-Free Wavelength Modulation Technology," *Chin. J. Lasers* **47**, 278–285 (2020).
19. M. Raza, L. Ma, S. Yao, L. Chen, and W. Ren, "High-temperature dual-species (CO/NH₃) detection using calibration-free scanned-wavelength-modulation spectroscopy at 2.3 μm ," *Fuel* **305**, 121591 (2021).
20. K. Levenberg, "A method for the solution of certain non-linear problems in least squares," *Q. Appl. Math.* **2**, 164–168 (1944).